



The first supramolecular-assembling structure of $[\text{Pb}^{\text{II}} \{ \text{O}_2\text{N}(\text{C}_6\text{H}_4)\text{NNN}(\text{O})\text{Ph} \}_2]$ through metal– η^6 arene π -interactions: Synthesis and X-ray characterization of aryl-substituted triazenide lead(II) complex

Bernardo A. Iglesias, Davi Fernando Back*, Manfredo Hörner*, Estela R. Crespan, Fernanda Broch

Departamento de Química, Universidade Federal de Santa Maria (UFSM), 97105-900 Santa Maria, RS, Brazil

ARTICLE INFO

Article history:

Received 31 October 2013

Received in revised form

22 November 2013

Accepted 28 November 2013

Keywords:

Triazene 1-oxide

Lead complexes

Pb– η^6 arene π -interaction

ABSTRACT

$\text{Pb}(\text{SCN})_2$ reacts with metallic sodium (Na^0) 1-phenyl-3-(4-nitrophenyl) triazene 1-oxide in tetrahydrofuran, leading to the formation of orange-colored crystals of the $[\text{Pb}^{\text{II}} \{ \text{O}_2\text{N}(\text{C}_6\text{H}_4)\text{NNN}(\text{O})\text{Ph} \}_2]$ complex, which is the first lead (Pb(II)) complex with reciprocal metal– η^6 arene π -interactions. The crystal structure belongs to the monoclinic space group $P2_1/n$ and the lattice of $[\text{Pb}^{\text{II}} \{ \text{O}_2\text{N}(\text{C}_6\text{H}_4)\text{NNN}(\text{O})\text{Ph} \}_2]$ can be viewed as a unidimensional supramolecular assembling of $[\text{Pb}^{\text{II}} \{ \text{O}_2\text{N}(\text{C}_6\text{H}_4)\text{NNN}(\text{O})\text{Ph} \}_2]$ units linked through intermolecular metal–arene π -interactions.

© 2013 Elsevier B.V. All rights reserved.

1. Introduction

It is well known that secondary bonds, or interactions, can play a significant role in the structural assembling of a wide variety of compounds. These interactions present σ or π characteristics but have not been recognized in earlier works, in spite of their real existence [1–3].

As a heavy *p*-block metal ion, lead (II) possesses a large radius, variable stereochemical activity, and a flexible coordination environment, which provides unique opportunities for the construction of a novel network of topologies and interesting properties. Consequently, the mechanisms of Pb(II) ions binding to domains have been extensively studied, using various techniques. In these investigations, the Pb(II) coordination chemistry, such as lone pair of electrons, coordination number, and coordination geometry, plays an important role in the elucidation of the interactions of lead ions. Additionally, the study of Pb(II) model complexes in biological systems and the removal of lead by chelating agents through coordination, have been of crucial importance [4,5].

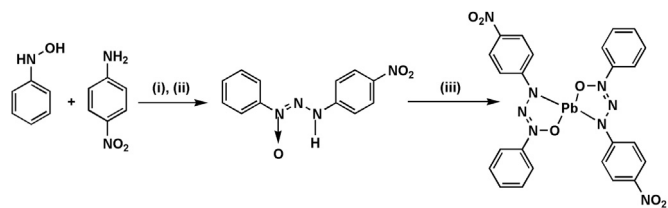
* Corresponding authors. Tel.: +55 55 3220 8056; fax: +55 55 3220 8031.

E-mail addresses: davifback@cnpq.br, davifback@gmail.com (D.F. Back), hoerner@smail.ufsm.br (M. Hörner).

On the other hand, the Pb(II) ion can exhibit a variable coordination number and geometry, with or without a stereochemically active lone pair. Therefore, structural diversities in lead complexes will inevitably occur, as shown in this study. Coordination bounds and non-covalent interactions such as hydrogen bonding and π – π interactions [6,7], the metal-to-ligand molar ratio, the coordinative function of the ligand, the type of metal ions, the presence of the solvent molecules, counterions or organic guest molecules, and interactive information stored in the ligands, should all be taken into account in the process of rational design and synthesis of metal coordination polymers [8–10].

According to the literature [11–13], a *tecton* is defined as any molecule whose interactions are dominated by particular associative forces that induce the self-assembling of an organized network with specific architectural or functional features.

In this article we present the first Pb(II) triazenide complex containing tectons with the strategic capability of self-assembly via metal– η -arene π interactions. Another similar example of tectons using the metal mercury $\{[\text{RC}_6\text{H}_4\text{NNNC}_6\text{H}_4\text{R}]_2(\text{Py})\}$, where (*R* = *m*-acetyl), showed a difference – in this case it was due to the metal being complexed with phenyl-triazene chain links and metal– η^2 π -arene interactions occurring [14] proving that such interactions also play an important role in the architecture of the crystal lattice [15–17].



(i) NaNO₂, HCl, 0–5 °C; (ii) H₂O, NaCOOCH₃; (iii) Pb(SCN)₂, Na⁺, THF, MeOH, pyridine

Scheme 1. Synthesis of free ligand and lead(II) complex, respectively.

2. Experimental section

2.1. Preparation of the ligand 1-phenyl-3-(4-nitrophenyl) triazene 1-oxide

4-Nitroaniline (0.5 g, 3.62 mmol) was dissolved in a mixture of 15 mL of concentrated HCl and 5 mL of distilled water and the system was cooled to between 0 °C and 5 °C. Then NaNO₂ (0.300 g, 4.34 mmol) was added under constant stirring. After 30 min stirring, an acid solution of β-phenylhydroxylamine (0.39 g, 3.62 mmol in CH₃COOH) was added and the medium was neutralized to a pH of around 6.00, with a solution of NaCOOCH₃. The yellow precipitate was filtered under vacuum and washed several times with cold water and then crystallized with anhydrous EtOH (**Scheme 1**). Yield of 86% (3.1 mmol) based on 4-nitroaniline taken.

Table 1

Crystal data and structure refinement of the ligand 1-phenyl-3-(4-nitrophenyl) triazene 1-oxide, and the complex [Pb^{II}{O₂N(C₆H₄)NNN(O)Ph}₂].

Empirical formula	C ₁₂ H ₁₀ N ₄ O ₃	C ₃₂ H ₂₄ N ₁₁ O ₈ Pb
Formula weight	258.24	721.65
T (K)	293(2)	293(2)
Radiation, λ (Å)	0.71013	0.71013
Crystal system,	Monoclinic, P2 ₁ /c	Monoclinic, P2 ₁ /n
Space group		
Unit cell dimensions		
a (Å)	13.073(5)	17.4967(2)
b (Å)	7.006(5)	8.0036(10)
c (Å)	13.116(5)	18.1148(3)
α (°); γ (°)	90	90
β (°)	93.74(5)	102.789(10)
Volume (Å ³)	1198.7(9)	2473.8(6)
Z, calculated	4, 1.431	4, 1.938
density (g cm ⁻³)		
Absorption	0.107	6.878
coefficient (mm ⁻¹)		
F(000)	536	1392
Crystal size (mm)	0.16 × 0.11 × 0.01	0.13 × 0.085 × 0.056
θ Range (°)	3.30–25.50	2.81–28.78
Limiting indices	–15 ≤ h ≤ 15, –8 ≤ k ≤ 8, –15 ≤ l ≤ 15	–21 ≤ h ≤ 23, –10 ≤ k ≤ 10, –24 ≤ l ≤ 24
Reflections	11873/2205	52536/6398
collected/unique	[R(int) = 0.0453]	[R(int) = 0.0475]
Completeness	98.8%	99.5%
to theta max.		
Max. and min.	0.92143 and 0.832247	0.95275 and 0.839387
transmission		
Absorption correction	Gaussian	Gaussian
Refinement method	Full-matrix	Full-matrix
	least-squares on F ²	least-squares on F ²
Goodness-of-fit on F ²	0.966	1.006
Data/restraints/	2205/0/173	6398/0/352
parameters		
Final R indices	R1 = 0.0441, wR2 = 0.1034	R1 = 0.0281, wR2 = 0.0425
[I > 2σ(I)]		
R indices (all data) ^a	R1 = 0.0978, wR2 = 0.1244	R1 = 0.0551, wR2 = 0.0480
Largest diff. peak	0.156–0.120	0.739–0.821
and hole (e Å ⁻³)		

^a R₁ = |F_o – F_c|/|F_o|; wR² = [w(F_o² – F_c²)²/(wF_o²)]^{-1/2}.

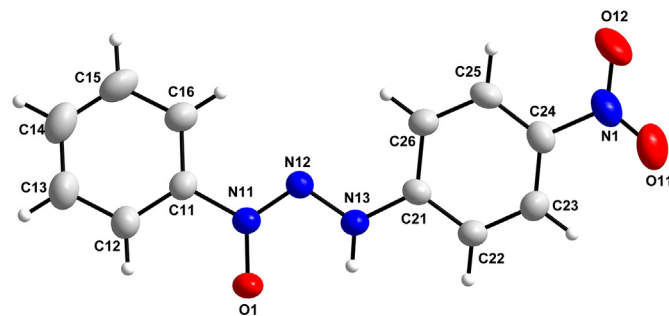


Fig. 1. Molecular structure of N-oxide ligand with 40% thermal ellipsoids (using DIAMOND software [15]).

Properties: yellow crystals of C₁₂H₁₀N₄O₃ (258.08 g mol⁻¹); and melting point of 180 °C–182 °C. IR (KBr) free ligand 1-phenyl-3-(4-nitrophenyl) triazene: 3200 [s, ν(N–H)]; 1298 [s, ν(N→O)]; 1225 [s, ν(N–N)]; and 1470 [s, ν(N=N)]. Ultraviolet–visible (EtOH, qualitative analysis) free ligand 1-phenyl-3-(4-nitrophenyl) triazene in λ(nm): 393 [n→π*, N=N]; 265 [n→σ*, NNN]; and 202 [π→π*, C=C_{aromatic}]. ¹H NMR (400.0 MHz) in DMSO-d₆ free ligand, with values in δ (ppm): 11.98 (s, 1H, OH); 8.09 (d, 2H, J = 8.0 Hz); 7.57 (d, 2H, J = 7.6 Hz); 7.37 (d, 2H, J = 8.0 Hz); 7.04 (dd, 3H, J = 7.7 Hz).

2.2. Preparation of the complex [Pb^{II}{O₂N(C₆H₄)NNN(O)Ph}₂] bis-1-phenyl-3-(4-nitrophenyl) triazene 1-oxide lead(II)

We performed all the manipulations in nitrogen, using standard Schlenk techniques. Small scrapings of Na⁰ were added

Table 2

Selected bond lengths [Å] and angles [°] for the 1-phenyl-3-(4-nitrophenyl) triazene 1-oxide compounds and the [Pb^{II}{O₂N(C₆H₄)NNN(O)Ph}₂] complex.

1-Phenyl-3-(4-nitrophenyl) triazene 1-oxide ligand		[Pb ^{II} {O ₂ N(C ₆ H ₄)NNN(O)Ph} ₂] complex	
Bond lengths (Å)		Bond lengths (Å)	
N(12)–N(13)	1.332(2)	O(2)–Pb	2.389(2)
N(12)–N(11)	1.232(2)	O(12)–N(1)	1.216(5)
N(11)–O(1)	1.284(2)	C(11)–N(11)	1.404(4)
N(11)–C(11)	1.440(2)	C(21)–N(13)	1.445(4)
N(13)–C(21)	1.386(2)	C(31)–N(21)	1.436(4)
N(1)–C(24)	1.457(3)	C(41)–N(23)	1.413(4)
N(1)–O(11)	1.232(2)	N(1)–O(11)	1.219(4)
N(1)–O(12)	1.225(2)	N(11)–N(12)	1.324(3)
N(13)–H(1)	0.861(2)	N(11)–Pb	2.391(3)
		N(12)–N(13)	1.283(3)
		N(13)–O(1)	1.317(3)
		N(21)–N(22)	1.289(3)
		N(22)–N(23)	1.320(3)
		N(23)–Pb	2.432(3)
		O(1)–Pb	2.358(2)
Bond angles (°)		Bond angles (°)	
O(12)–N(1)–O(11)	123.7(2)	N(21)–O(2)–Pb	112.95(15)
O(12)–N(1)–C(24)	118.3(2)	C(42)–C(41)–N(23)	124.4(3)
O(11)–N(1)–C(24)	118.0(2)	O(12)–N(1)–O(11)	123.6(4)
N(12)–N(11)–O(1)	122.55(16)	N(12)–N(11)–Pb	116.89(18)
N(12)–N(11)–C(11)	117.46(16)	N(13)–N(12)–N(11)	113.9(2)
O(1)–N(11)–C(11)	119.95(17)	N(12)–N(13)–O(1)	123.0(2)
N(11)–N(12)–N(13)	112.04(15)	N(22)–N(21)–O(2)	122.7(2)
N(12)–N(13)–C(21)	119.74(16)	N(21)–N(22)–N(23)	113.3(2)
N(12)–N(13)–H(13A)	120.1	N(13)–O(1)–Pb	113.82(16)
C(21)–N(13)–H(13A)	120.1	O(1)–Pb–O(2)	136.04(7)
		O(1)–Pb–N(11)	64.60(8)
		O(2)–Pb–N(11)	83.46(8)
		O(1)–Pb–N(23)	81.97(7)
		O(2)–Pb–N(23)	63.28(8)
		N(11)–Pb–N(23)	81.57(8)

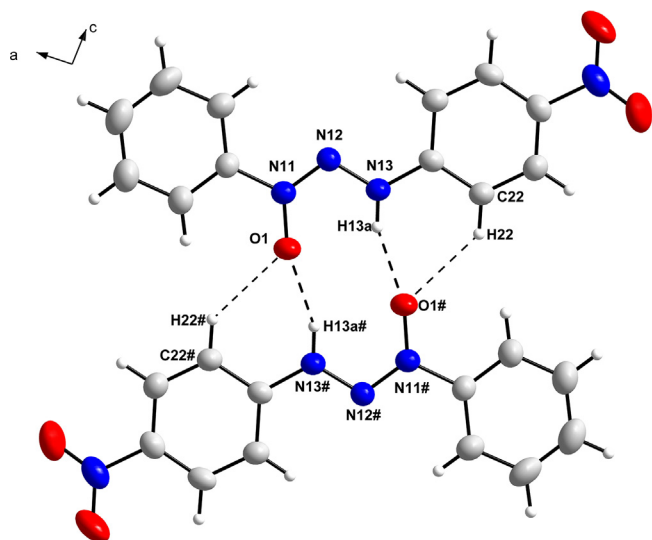


Fig. 2. Section of the extended one-dimensional tecton of the N-oxide ligand with 40% thermal ellipsoids (using DIAMOND software [20]). Symmetry operations used to generate equivalent atoms: (#) $1 - x, -y, -z$.

under stirring to a solution of 0.03 g (0.116 mmol) of 1-phenyl-3-(4-nitrophenyl) triazene 1-oxide in 20 mL of THF. To the dark-purple solution of the deprotonated ligand, 0.018 g (0.058 mmol) of $\text{Pb}(\text{SCN})_2$ was dissolved in 5 mL of absolute MeOH. After 1 h, 2 g of anhydrous MgSO_4 was added and the mixture was stirred for an additional 20 min. The mixture was filtered and the solvent was evaporated. The residual orange solid was dissolved in an absolute mixture of methanol/pyridine (10:2 v/v) see Scheme 1. Prismatic light-orange crystals were obtained within three days after slow evaporation of the solvent at room temperature. Yield of 60% (0.034 mmol) based on triazene taken.

Properties: prismatic light-orange crystalline substance – $\text{C}_{24}\text{H}_{18}\text{N}_8\text{O}_6\text{Pb}$ (721.65 g mol⁻¹) and melting point of 290 °C. IR (KBr) lead(II) triazenide complex: 1222 [s, $\nu(\text{N} \rightarrow \text{O})$]; 1107 [s, $\nu(\text{N} - \text{N})$]; 1334 [s, $\nu(\text{NO}_2)$]; and 1311 [vs, $\nu(\text{NNN})$] – the $\nu(\text{N} - \text{H})$ is absent. Ultraviolet–visible (EtOH, qualitative analysis) in $\lambda(\text{nm})$: 386 [$n \rightarrow \pi^*$, $\text{N} = \text{N}$], 250 [$n \rightarrow \sigma^*$, NNN]. ¹H NMR (400.0 MHz) in $\text{DMSO}-d_6$ lead(II) triazenide complex, with values in δ (ppm): 8.27 (d, 2H, $J = 8.1$ Hz); 8.16 (d, 2H, $J = 7.6$ Hz); 7.70 (d, 2H, $J = 8.1$ Hz); and 7.61 (dd, 3H, $J = 7.5$ Hz).

3. Crystallography

Data were collected using a Bruker APEX II CCD area-detector diffractometer and employing graphite-monochromatized $\text{MoK}\alpha$ radiation. The structures from the ligand and the complex were solved by direct methods using SHELXS-97 [18]. Subsequent Fourier-difference map analyses yielded the positions of the non-hydrogen atoms. Refinements were done with the SHELXL-97 package [19]. All refinements were done by full matrix least-

Table 3
Secondary interactions: lengths (Å) and angles (°) for N-oxide ligand complex.

D–H...A ^a	D–H	H...A	D...A	D–H...A
N13–H1...O1 ^b	0.861(3)	2.185(1)	2.957(2)	149.15(11)
C26–H26...O3 ^b	0.930(2)	2.570(1)	3.304(3)	136.10(13)

^a D = donor and A = acceptor. Symmetry operations used to generate equivalent atoms.

^b $1 - x, -y, -z$.

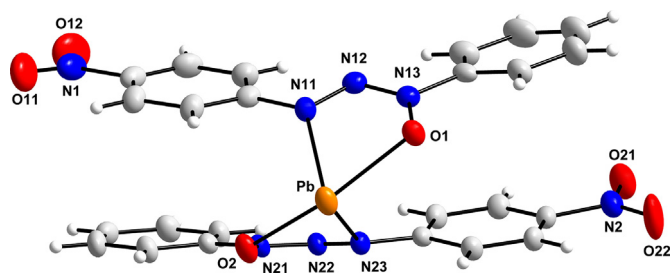


Fig. 3. The molecular structure with the atom-labeling scheme of the $[\text{Pb}^{\text{II}}\{\text{O}_2\text{N}(\text{C}_6\text{H}_4)\text{NNN}(\text{O})\text{Ph}\}_2]$ with 40% thermal ellipsoids (using DIAMOND software [20]).

squares on F2, with anisotropic displacement parameters for all non-hydrogen atoms. Hydrogen atoms were included in the refinement in calculated positions. Drawings were done using DIAMOND for Windows [20]. Crystal data and more details of the data collection and refinements are contained in Table 1.

4. Results and discussion

4.1. Crystal structure

The ligand triazene-1-oxide was synthesized from a classical diazotization reaction [21,22]. The crystal structure of the N-oxide ligand consists of atoms of an organic molecule with the functional diazoamino group $\text{N11}=\text{N12}-\text{N13}$ featuring an asymmetric triazene, the molecule is composed of aromatic rings linked to the terminal nitrogens (N11 and N13). The ring attached to the terminal nitrogen N13 has a nitro function ($-\text{NO}_2$) and the other ring attached to the terminal nitrogen N11 is presented only as a phenyl ring (Fig. 1).

The length of the $\text{N12}-\text{N13}$ bond [1.333(2) Å] is less than the characteristic value for a single $\text{N}-\text{N}$ bond (1.44 Å), while the length of the $\text{N11}-\text{N12}$ bond [1.276(2) Å] is larger than the bond length for a typical $\text{C}=\text{N}$ double bond (1.24 Å). All these afore mentioned values indicate that the bonds have a partial double-bond character, implying a relocation of the π electrons in the chains $\text{N11}-\text{N12}=\text{N13}$ (selected distances and angles are discussed in Table 2).

Observing the packing of the molecule, one can see that the H13A atom of the triazene chain produces intermolecular interactions with forked receptor geometry ($\text{D1}, \text{H1}, \text{H2}, \text{D2}\cdots\text{A}$ ($\text{D} = \text{donor atom}, \text{A} = \text{receptor atom}$) [21,23] [16,18]. Consequently, the molecules of the triazene are related via these connections. The atoms considered to be donor atoms are N13 ($\text{H13A}-\text{N13}$) and C22 ($\text{C22}-\text{H22}$), where as the receptor is the O1 oxygen atom of the N-oxide function (Fig. 2). Distances and angles are described in Table 3.

Crystal data and the experimental conditions for $[\text{Pb}^{\text{II}}(\text{RC}_6\text{H}_4\text{NNNC}_6\text{H}_5)_2]$ ($R = p\text{-NO}_2$) are given in Table 1. Selected bond distances and angles are listed in Table 2 and Fig. 3 shows the molecular structure of the single complex in a thermal ellipsoid representation with 40% thermal ellipsoids (using DIAMOND software [20]).

In a single complex, two deprotonated 1,3-diaryl-substituted triazenide ligands are inversely coordinated to one $\text{Pb}(\text{II})$ ion by means of two primary $\text{Pb}-\text{N}$ bonds and two primary $\text{Pb}-\text{O}$ interactions (Fig. 3). The asymmetric unit is formally related with just two molecules of the ligand and the $\text{Pb}(\text{II})$ ion. Thus, the complex is not planar, but has highly distorted quadratic geometry.

The translation operated moieties are stacked unidimensionally along the crystallographic b axis through $\text{Pb}-\eta^6\text{-arene}$ π interactions between the $\text{Pb}(\text{II})$ ion and carbons atoms of the phenyl rings of neighboring complexes.

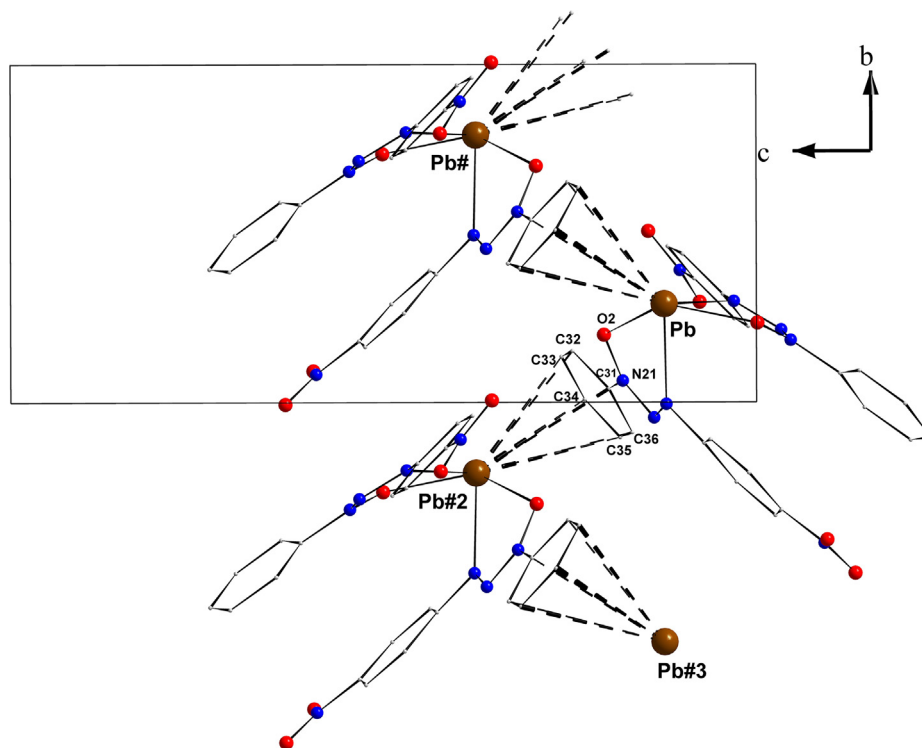


Fig. 4. View of the supramolecular 1-D assembling of $[\text{Pb}^{\text{II}}\{\text{O}_2\text{N}(\text{C}_6\text{H}_4)\text{NNN}(\text{O})\text{Ph}\}_2]$ along the $[010]$ direction via $\text{Pb}(\text{II})-\eta^6$ -arene π -interactions (indicated as dashed lines). Symmetry operations used to generate equivalent atoms: (#) $1.5 - x, 0.5 + y, 0.5 - z$; (#2) $1.5 - x, -0.5 + y, 0.5 - z$; (#3) $x, -1 + y, z$.

Like the $\text{Pb}-\eta^6$ -arene π interactions, the phenyl rings of the metallocene are located apical to the main molecular plane of the $\text{Pb}(\text{II})$ lead atom. The two triazenide chains are linked toward one metallic center, above and below the plane, reinforcing the chaining of the lattice. Thus, six carbon atoms of the C31 to C36 ring have remarkably short distances to the $\text{Pb}(\text{II})$ ion: the shortest

intermolecular distances from the $\text{Pb}(\text{II})$ centers toward the phenyl rings are 3.792(3) Å [$\text{Pb}\#2-\text{C}31$]; 3.684(0) Å [$\text{Pb}\#2-\text{C}32$]; 3.634(1) Å [$\text{Pb}\#2-\text{C}33$]; 3.677(2) Å [$\text{Pb}\#2-\text{C}34$]; 3.763(2) Å [$\text{Pb}\#2-\text{C}35$]; 3.820(1) Å [$\text{Pb}\#2-\text{C}36$]; and symmetry code (#2) [$1.5 - x, -0.5 + y, 0.5 - z$]. The distance from the metallic ion to the midpoint of the center of the phenyl ring is 3.457 Å (Fig. 4).

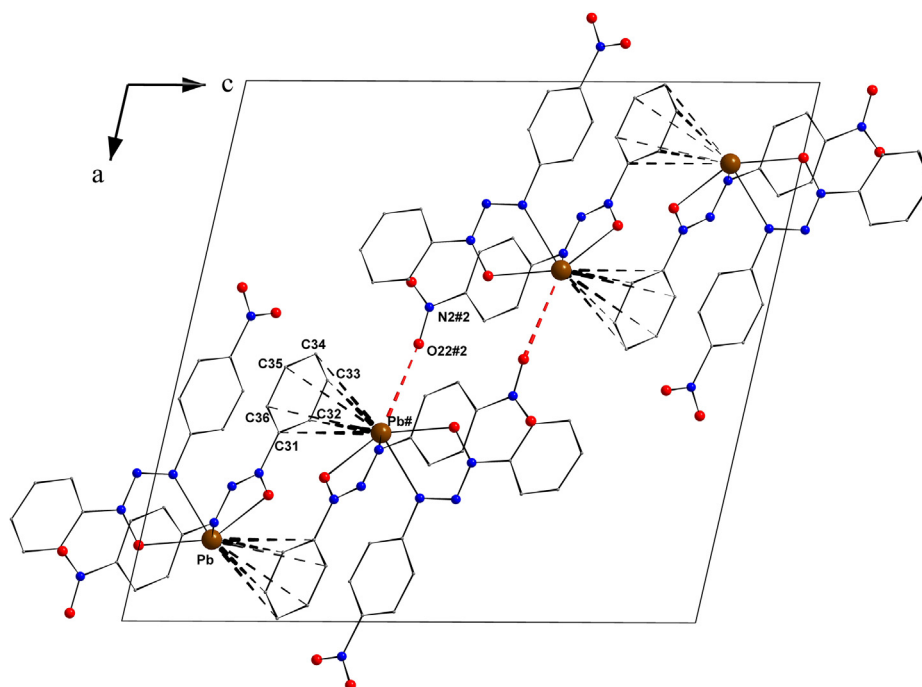


Fig. 5. Representation of the $\text{Pb}\#-\text{O}22\#2-\text{N}2\#2$ interaction along the crystallographic ac plane (dashed red line). Symmetry operations used to generate equivalent atoms: (#) $1.5 - x, -0.5 + y, 0.5 - z$; (#2) $-0.5 + x, -0.5 - y, 0.5 + z$. (For interpretation of the references to colour in this figure legend, the reader is referred to the web version of this article.)

The difference in the distances between the connecting carbon atoms of the aromatic ring and the metal center showed that there is a tendency to approach for atoms C32, C33, and C34 and a substantial distance from the metal center and the C31, C35, and C36 atoms.

This difference, which indicates as light distortion, can be justified because of the strong interaction (compared with the π - η^6 -aryl interactions) of oxygen atoms from then nitro functions and the metal center: 3.188(1) Å [Pb#–O22#2] and 165.28(1)° [Pb#–O22#2–N2#2]; symmetry code (#) 1.5 – x, –0.5 + y, 0.5 – z; (#2) –0.5 + x, –0.5 – y, 0.5 + z; as shown in Fig. 5.

The η^6 -arene interactions are cited in the literature in organometallic or transition metals complexes [24,25] and justifications for such interactions are discussed, among which we mention the study of Zenneck, U. and collaborators [26]. According to this article this type of interaction is caused by intramolecular interactions and the chiral stereochemistry groups.

This approach is very applicable for the above example [26] however, in the case of the lead complex we need to evaluate the steric effects in addition to crystal packing, because there is supramolecular assembling. Situation that does not occur in the case of complex synthesized by Frank [27], because in this case there is a monomeric arene lead (II).

Structural modification of the ligand by changing the steric bulk of the substituents as well as the investigation of crystallization processes are basic requirements for the future prospects of work, only then, can we corroborate the results proposed by Zenneck, U. and collaborators [26].

5. Conclusions

The synthesis of this triazene N-oxide was very effective for promoting complexing to the metal center. Despite the nitro function being present in the triazene 1-oxide binder, the binder had a direct influence on the steric and electronic structure of the complex and provided unexpected interactions during the preparation of the synthesis, but corroborated the first report in the literature of a Pb- η^6 -arene π interaction. The triazene used in this work was very important for finding preliminary evidence and will enable us to select the best data to search for new, specific interactions.

Acknowledgments

This work was supported by the Brazilian National Research Council (CNPq) – Edit. No. 14/2011; and FAPERGS (Fundação de Amparo à Pesquisa do Estado do Rio Grande do Sul) – Edit. No. 002/2011-PqG.

Appendix A. Supplementary data

CCDC 952360 and 952361 contain the supplementary crystallographic data for this paper. These data can be obtained free of charge from The Cambridge Crystallographic Data Centre via www.ccdc.cam.ac.uk/data_request/cif.

References

- [1] M. Hörner, G.M. Oliveira, E.G. Koehler, L.C. Visentin, *J. Organomet. Chem.* 691 (2006) 1311–1314.
- [2] M. Hörner, G.M. Oliveira, L. Bresolin, A.B. Oliveira, *Inorg. Chim. Acta* 359 (2006) 4631–4634.
- [3] M. Hörner, F. Broch, L.C. Visentin, *Z. Anorg. Allg. Chem.* 633 (2007) 1779–1782.
- [4] J. Yang, J.F. Ma, Y.Y. Liu, J.C. Ma, S.R. Batter, *Inorg. Chem.* 46 (2007) 6542–6555.
- [5] Q. Y. Liu, L. Xu, *Eur. J. Inorg. Chem.* 8 (2006) 1620–1628.
- [6] M. Hörner, B.A. Iglesias, P.R. Martins, P.C.M. Villis, L.C. Visentin, *Z. Anorg. Allg. Chem.* 634 (2008) 1058–1062.
- [7] M. Hörner, B.A. Iglesias, P.R. Martins, P.C.M. Villis, *X-Ray Struct. Anal.* 24 (2008) x123–x124.
- [8] S.R. Fan, L.G. Zhu, *Inorg. Chem.* 46 (2007) 6785–6793.
- [9] A.A. Danopoulos, K.Y. Monakhov, V. Robert, P. Braunstein, R. Pattacini, S. Conde-Guadano, M. Hanton, R.P. Tooze, *Organometallics* 32 (2013) 1842–1850.
- [10] H.A. Burkill, R. Vilar, A.J.P. White, *Inorg. Chim. Acta* 359 (2006) 3709–3722.
- [11] P. Grosshans, A. Jouaiti, V. Bulach, J. Planeix, M.W. Hosseini, J. Nicoud, C. R. Chim. 7 (2004) 189–196.
- [12] Y.L. Chang, M. West, F.W. Fowler, J.W. Lauher, *J. Am. Chem. Soc.* 115 (1993) 5991–6000.
- [13] P. Dechambenoit, S. Ferlay, M.W. Hosseini, *Cryst. Growth Des.* 5 (2005) 2310–2312.
- [14] M. Hörner, G.M. Oliveira, J.A. Naue, J. Daniels, J. Beck, *J. Organomet. Chem.* 691 (2006) 1051–1054.
- [15] M.C.T. Fyfe, J.F. Stoddart, *Acc. Chem. Res.* 30 (1997) 393–401.
- [16] R. Sharma, G.N. Pandey, S.N. Sharma, R. Ranjan, P. Kumar, *Asian J. Chem.* 7 (1995) 147–150.
- [17] R.P. Sharma, A. Singh, P. Venugopalan, G. Yanan, J. Yu, C. Angeli, V. Ferretti, *Eur. J. Inorg. Chem.* 2012 (2012) 1195–1203.
- [18] G.M. Sheldrick, *SHELXS-97: Program for Crystal Structure Solution*, University of Göttingen, Germany, 1997.
- [19] G.M. Sheldrick, *SHELXL-97: Program for Crystal Structure Refinement*, University of Göttingen, Germany, 1997.
- [20] K. Brandenburg, *DIAMOND 3.1a*, Crystal Impact GbR, Bonn, Germany, 1997–2005. Version 1.1a.
- [21] D. F. Back, M. Hörner, F. Broch, G.M. Oliveira, *Polyhedron* 31 (2012) 558–564.
- [22] G.M. Oliveira, M. Hörner, A. Machado, D.F. Back, J.H.S.K. Monteiro, M.R. Davolos, *Inorg. Chim. Acta* 366 (2011) 203–208.
- [23] D.F. Back, C.R. Kopp, G.M. Oliveira, P.C. Piquini, *Polyhedron* 36 (2012) 21–29.
- [24] M.P. Boone, D.W. Stephan, *J. Am. Chem. Soc.* 135 (2013) 8508–8511.
- [25] M. Patra, K. M. N. Metzler-Nolte, *Dalton Trans.* 41 (2012) 112–117.
- [26] F. Heinemann, J. Klodwig, F. Knoch, M. Wundisch, U. Zenneck, *Chem. Ber. Recueil.* 30 (1997) 123–130.
- [27] W. Frank, F.-G. Wittmer, A. Monomeric Bis, *Eur. J. Inorg. Chem.* 130 (12) (1997) 1731–1732.